LA-UR-. 96-4788

CONF-9605253--1

Approved for public release; distribution is unlimited.

Title: Antihydrogen production and precision experiments

Author(s):
M. Nieto/T-8
T. Goldman/ T-5
M. Holzscheiter/ P Division
R. Hughes/ P Division
N. King/ P Division
G. Morgan/ P Division

Submitted to: Proceedings of the "Third Biellial Conference on Low Energy Antiproton Physics" held near Rome, 19-25 May, 1996

DISCLAIMER

Los Alamos
NATIONAL LABORATORY

Antihydrogen production and precision experiments

M. H. Holzscheiter [a] *, G. Bendiscioli[b], A. Bertin[c], G. Bollen[d], M. Bruschi[c], C. Cesar[e], M. Charlton[f], M. Corradini[g], D. DePedis[h], M. Doser[d], J. Eades[d], R. Fedele[i], X. Feng[d†], F. Galluccio[i], T. Goldman[a], J. S. Hangst[j], R. Hayano[k], D. Horváth[d†], R. J. Hughes[a], N. S. P. King[a], K. Kirsebom[j], H. Knudsen[j], V. Lagomarsino[l], R. Landua[d], G.Laricchia[f], R. A. Lewis[m], E. Lodi-Rizzini[g], M. Macri[l], G. Manuzio[l], U. Marconi[c], M. R. Masullo[i], J. P. Merrison[j], S. P. Møller[j], G. L. Morgan[a], M. M. Nieto[a], M. Piccinini[c], R. Poggiani[n], A. Rotondi[b], G. Rouleau[d†], P. Salvini[b], N. Semprini-Cesari[c], G. A. Smith[m], C. M. Surko[o], G. Testera[l], G. Torelli[n], E. Uggerhøj[j], V. G. Vaccaro[i], L. Venturelli[g], A. Vitale[c], E. Widmann[d], T. Yamazaki[k], Y. Yamazaki[k], D. Zanello[h], A. Zoccoli[c]

[a]Los Alamos National Laboratory, Los Alamos, New Mexico 87545, U.S.A.

[b]Pavia University & INFN , Pavia, Italy

[c]Bologna University & INFN, Bologna, Italy

[d]CERN, CH1211 Geneva, Switzerland

[e]Escola Tecnica Federal do Ceara, Fortaleza, CE 60040-531, Brazil

[f]Dept. of Physics & Astronomy, University College London, London, WC1E6BT, UK

[g]Brescia University & INFN , Brescia, Italy

[h]Rome University "La Sapienza" & INFN , Rome, Italy

[i]Napoli University & INFN, Mostra d'Oltremare Pad. 20, I-80125 Napoli, Italy

[j]Inst. for Physics & Astronomy, University of Aarhus, DK-8000 Aarhus C, Denmark

[k]University of Tokyo, Tokyo, Japan

[l]Genoa University & INFN, Via Dodecaneso 33, I-16146 Genoa, Italy

[m]Pennsylvania State Univ., 303 Osmond Laboratory, University Park, PA 16802, U.S.A.

[n]Pisa University & INFN, I-56100 Pisa, Italy

[o]University of California at San Diego, La Jolla, CA 92093-0319, U.S.A.

The study of CPT invariance with the highest achievable precision in all particle sectors is of fundamental importance for physics. Equally important is the question of the gravitational acceleration of antimatter. In recent years, impressive progress has been achieved in capturing antiprotons in specially designed Penning traps, in cooling them to energies of a few milli-electron volts, and in storing them for hours in a small volume of space. Positrons have been accumulated in large numbers in similar traps, and low energy positron or positronium beams have been generated. Finally, steady progress has been made in trapping and cooling neutral atoms. Thus the ingredients to form antihydrogen at rest are at hand. Once antihydrogen atoms have been captured at low energy, spectroscopic methods can be applied to interrogate their atomic structure with extremely high precision and compare it to its normal matter counterpart, the hydrogen atom. Especially the 1S-2S transition, with a lifetime of the excited state of 122 msec and thereby a natural linewidth of 5 parts in 10^{16}, offers in principle the possibility to directly compare matter and antimatter properties at a level of 1 part in 10^{18}.

1. Introduction

CPT invariance is a fundamental property of quantum field theories in flat space-time, which results from the basic requirements of locality, Lorentz invariance and unitarity [1–5]. Principal consequences include the predictions that particles and their antiparticles have equal masses and lifetimes, and equal and opposite electric charges and magnetic moments. It also follows that the fine structure, hyperfine structure, and Lamb shifts of matter and antimatter bound systems should be identical.

A number of experiments have tested some of these predictions with impressive accuracy [6], e.g. with a precision of 10^{-12} for the difference between the moduli of the magnetic moment of the positron and the electron [7] and of 10^{-9} for the difference between the proton and antiproton charge-to-mass ratio [8]. However, the most stringent CPT test comes from a mass comparison of neutral kaon and antikaon, where the tremendous accuracy of 10^{-18} has been reached, albeit in a theoretically dependent manner.

Such a fundamental theorem must, of course, be tested as stringently as possible wherever feasible. In this regard, one may draw an analogy to M. Goldhaber's initial tests of baryon number violation, which is now understood to be by no means as significantly deep a principle as CPT. And indeed, pursuit of more vigorous tests of the baryon conservation law was not forthcoming before a theoretical context (Grand Unification) for its possible violation had been established. CPT violation is now on the threshold of a similar transition: from clearly important but with no concept of specific implications of its violation; to a deeper understanding of the significance, importance and physical mechanism for its violation [9–20].

The availability of antihydrogen atoms produced and stored at very low energies would offer new possibilities for a very precise comparison of matter and antimatter systems. In particular, the long lifetime (122 ms) of the metastable 2S level sets an ultimate limit for measuring the 1S-2S energy difference of 10^{-18}, if the line width can be reduced to the quantum limit [21], and if the centre of the spectral line is determined to one part in 10^3. For a more detailed discussion of these and related issues, see also ref. [22].

Any difference e.g. in the frequency of the 1S-2S transition would signal new physics. Such an exciting result may be due to CPT violation, but it could also stem from an anomalous red-shift because of a different gravitational interaction of matter and antimatter [23].

As a long term goal, a direct comparison of the gravitational acceleration of hydrogen and antihydrogen in the Earth's gravitational field can be envisaged [24]. Once the technique of cooling antihydrogen to the Dopper limit (3 mK) has been demonstrated, such ballistic measurements will become possible, albeit with a more moderate precision.

2. Experimental overview

Using the method developed at LEAR [8, 25], antiprotons can be captured in an electromagnetic field configuration known as a Penning trap, and cooled to sub-eV temperatures by electron cooling. We plan to accumulate 10^7 cold antiprotons from the Antiproton Decelerator (AD) [26] proposed at CERN in such a trap enclosed in a large diameter superconducting magnet.

Large numbers of positrons have been accumulated in similar field configurations. Our collaboration plans to use a system based upon the positron accumulator presently operated at the University of California in San Diego, in which 10^8 low energy positrons are routinely accumulated in a few minutes.

One of the major challenges will consist of bringing the antiprotons and positrons in close contact for a time sufficiently long to allow the recombination process to take place. To combine free positrons with the antiprotons it has been proposed to use nested Penning traps [27, 28], a combined RF/Penning trap configuration [29], or to inject a (pulsed or continuous) beam of low energy positronium atoms into stored antiprotons [30].

In the nested traps the oppositely charged an-

*Spokesperson, Email: holzscheiter@cern.ch
†Visitor at CERN

tiprotons and positrons are stored in two different potential wells in close proximity and are cooled to low energy. At the time of recombination these two clouds need to be merged while preserving their low temperature and high densities. While the theoretical rate for this process is attractively high, this method may present a number of serious challenges, and despite a number of experimental efforts, no recombination of electrons and protons into hydrogen has been observed to date.

In a combined radio-frequency (Paul) and Penning trap particles of opposite electric charge can be confined by using the Penning trap for one species (i.e. the proton) and the superimposed RF fields to store the other particle (i.e. the electrons). Such a trap has recently been demonstrated to hold electrons and protons for long times, but the main problem identified was the heating of the particles by the RF fields, prohibiting high densities and low temperatures, both essential ingredients for efficient recombination and subsequent confinement of the neutrals.

A third possibility to form antihydrogen consists of bringing the positron to the antiproton in the form of a neutral positronium atom. Here positrons injected into the recombination region as a beam would be converted into positronium atoms in close proximity to the trapped antiprotons. Accumulation in an external positron trap may be used to enhance the instantaneous intensity of the positron beam used for positronium generation in the trap to allow for better background discrimination.

Once antiprotons and positrons have been recombined, the confinement by the electric forces ceases and the antihydrogen atoms would escape, hit the nearest wall, and annihilate. To confine the produced antihydrogen atoms magnetic gradients interacting with their magnetic moment can be used. This requires superimposing a strong magnetic field gradient onto the constant field necessary for the Penning trap. Typically a combination of quadrupole coils (Ioffe bars) for radial confinement and Helmholtz coils for the axial confinement is used [31].

We plan to use a large diameter, cold bore, superconducting magnet to house the antiproton trap, the positron storage trap, and the actual recombination trap inside a completely sealed, cryogenic vacuum environment. These components will be located inside a separate vacuum system, which can be inserted and removed from the main solenoid without affecting its cryogenic performance, and which can be cooled to a temperature at or below 0.5 K using a ^{3}He dilution (or evaporative) refrigerator.

The magnet coils to superimpose the Ioffe-Pritchard-type trap [32] onto the homogeneous field will be mounted on the inside of the main solenoid, and will be thermally coupled to the main cryogenic bath. The well depth of the magnetic trap has been designed such that a significant fraction of the formed antihydrogen can be confined.

The necessary detectors to study the formation and subsequent annihilation of antihydrogen as a function of time after the injection of positrons and antiprotons, and also as a function of trap parameters (well depths of antiproton/positron traps, density of charged particle clouds, magnetic well depth, etc.) will be mounted in the space between the inner vacuum shell and the Ioffe-Pritchard trap coils. Finally, access is provided for laser beams to the neutral trap (for stimulated recombination, laser cooling, and for spectroscopy), and the space for a 121.5 nm photon detector to observe the 2P-1S fluorescence is foreseen.

Figure 1 shows a general lay-out of the central portion of the apparatus containing the antiproton capture trap, the recombination trap with superimposed neutral trap and detector system, and the final positron storage trap. These individual items will be discussed in more detail in the subsequent sections. The initial goal of our collaboration is to reproduce the precision demonstrated in hydrogen by the groups at MIT [33] and the MPI Munich [34]. Such a precision can be achieved with the system as described here and $\approx$ 1000 Atoms at 0.5 K in the magnetic trap.

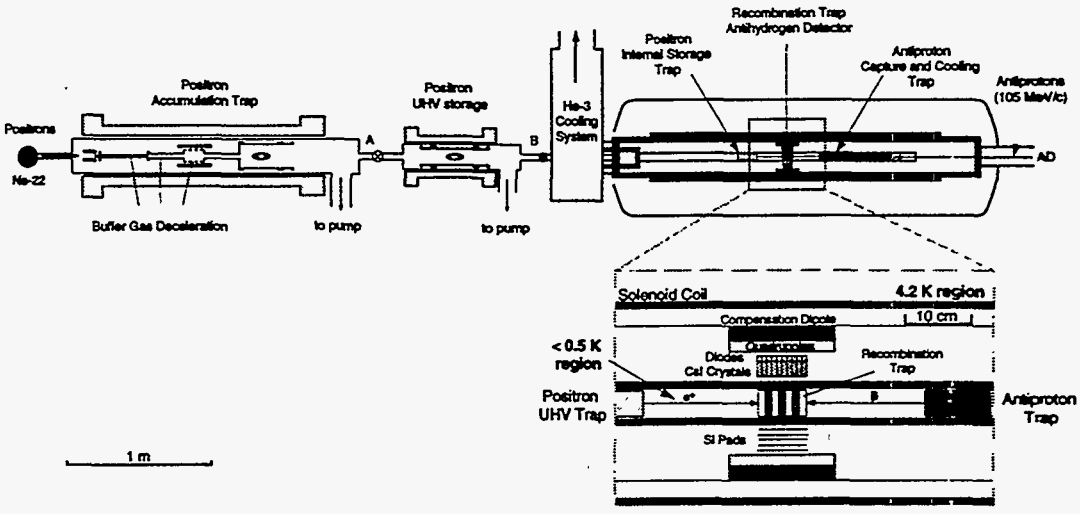

Figure 1. *Overview of the ATHENA apparatus showing the superconducting solenoid with the antiproton capture trap, the positron storage trap, and the recombination trap surrounded by the magnetic gradient trap.*

3. Capture and cooling of antiprotons

3.1. Current Status

The technique of capturing antiprotons into traps and cooling them to milli-eV energies has been developed at LEAR over the last 10 years [35,36]. The energy of a short pulse of antiprotons from LEAR (typically of 200 ns duration with a kinetic energy of 5.9 MeV) is degraded by a carefully optimized system of entrance counters and foils. The fraction of antiprotons exiting the last of these foils, which is an integral part of the trap structure, with energies below the trapping potential can then be dynamically captured by applying first a reflective voltage at the downstream electrode of the Penning trap, and then - before the reflected antiprotons leave the trap through the entrance electrode - rapidly ramping up to the full capture voltage.

The trap structure consists typically of seven electrodes: the entrance foil, a central region comprising five cylinders (two endcaps, two compensation electrodes, and the central ring), and a cylindrical high voltage exit electrode. The trap system is situated in the cryogenic bore of a superconducting solenoid capable of generating a magnetic field of up to 6 Tesla. The geometry of the central trap system is carefully chosen to produce a harmonic, orthogonalized quadrupole potential in the central region [37]. Its purpose is twofold: initially to store cold electrons, and then to collect the cooled antiprotons. Two experiments at LEAR have demonstrated trapping and cooling of antiprotons to sub-eV energies. PS 196 is using a small trap system of L =12 cm length and D = 1.2 cm diameter, and a capture voltage $U_c \approx 3$ kV. The dimensions are optimized for having precise control of the harmonic properties of the Penning trap, but the small trap size results in a capture efficiency of only 10^{-4}. The PS 200 system (L = 50 cm, D = 3.8 cm, $U_c \leq$ 30 kV) is designed to capture the largest possible number of antiprotons in this energy regime. Efficiencies of typically 0.5% are achieved, resulting in the capture of more than 10^6 antiprotons from a single LEAR bunch.

The initial kinetic energy of antiprotons after capture is in the keV range. Electron cooling is used to reduce the antiproton energy to values below 1 meV. For this purpose, a dense electron cloud is preloaded into the central region of the trap. These electrons cool to equilibrium with their cryogenic environment via synchrotron radiation. The antiprotons oscillate through the cold electron cloud and lose their energy via Coulomb collisions with a time constant of a few minutes. The efficiency observed for this process is better than 90% in both experiments. Owing to the very good vacuum within the cryogenic environment, the lifetime of cooled antiprotons reaches several hours or even months [38].

After the antiprotons have been cooled and stored in the central region of the trap, the capture potential at the entrance and exit electrodes can be switched off without losing antiprotons. Therefore it is possible to repeat the capture and cooling procedure several times, and both experiments have shown that this "stacking" allows increasing the number of stored antiprotons by a factor 10 or more. The enhancement figure was essentially limited by the number of LEAR shots obtainable without refilling the machine, and is expected to be much higher at the future AD, where many more pulses can be delivered to the experiments with a repetition rate of 1 pulse every 1 - 2 minutes.

3.2. Capture and cooling of antiprotons in ATHENA

The geometry of the ATHENA (ApparaTus for High precision Experiments on Neutral Antimatter) capture and cooling trap will be similar to the PS200 trap. It will be housed in a large bore solenoid (inner diameter $\geq$ 25 cm) with a homogeneous magnetic field ($\Delta B/B \leq 10^{-4}$) of about 3 Tesla over a 1.5 m long section. The inside of the bore is at a temperature of 4 K. The trap structure is further contained within a separate vacuum enclosure, which also accommodates the neutral (antihydrogen) trap and the internal positron storage trap. This enclosure is held at a temperature of 0.5 K or below and is completely separated from the magnet isolation vacuum and the outside by thin windows allowing injection of antiprotons and positrons. Owing to the very good vacuum (p $\leq 10^{-17}$ Torr) which can be

reached with such a completely sealed cryogenic system [38, 39], it is expected that very few antiprotons annihilate during a typical experimental cycle time of about 1 hour.

The AD will deliver 10^7 antiprotons per bunch, with a repetition rate of about 1 per minute. Assuming the theoretical capture efficiency for a 15 keV well depth of $\sim 1\%$ can be reached, 10^5 antiprotons would be trapped and cooled via electron cooling to cryogenic temperatures between two AD cycles. In order to reach the nominal goal of 10^7 cooled antiprotons, about 100 AD shots would have to be stacked in the trap.

The cooling of the antiprotons will use the well-known techniques developed at LEAR. A harmonic well in the middle of the trap is pre-loaded with $\approx 10^9$ electrons, which will reach thermal equilibrium with the 0.5 K environment via synchrotron damping within a few seconds at the magnetic field to be used.

Once a sufficient number of antiprotons (i.e. 10^7) has been accumulated and cooled, these may be transferred from the catching trap to the neutral trap. Both traps being situated inside a common solenoidal field, the transfer will be very efficient, since the problem of transporting very low energy antiprotons through magnetic fringe fields is not an issue. The temperature of the antiproton cloud will also not be affected during the transfer, provided the applied DC voltages have a stability of 0.1 mV or better.

4. Positron production and accumulation

Controlled sources of low energy positrons, and their efficient conversion to positronium atoms in vacuum, are readily available (for reviews see e.g. [40, 41]). Positrons emitted from radioactive sources, or in pair production from bremsstrahlung, usually have a wide range of kinetic energies in the MeV region and upon penetrating solid matter slow typically within a few picoseconds to an energy close to the thermal level. Once slowed the positron is free to diffuse in the medium (in which most annihilate), with a diffusion length around $10^3 - 10^4$ Å and dependent upon the moderating material. During the diffusion process a positron may encounter again the surface of the solid and be spontaneously emitted into the surrounding vacuum as a free positron, or bound to an electron as positronium. Comparing the penetration depth of the positron with its diffusion length immediately gives some idea of the efficiency of moderation (i.e. the production efficiency of slow positrons in vacuum from an initially energetic ensemble incident upon the material). This is around 10^{-3} for positrons from a radioactive source, but is typically lower for the more energetic positrons from pair production.

When low energy positrons are incident upon surfaces in vacuum they can be re-emitted as positrons or positronium atoms under conditions which can be controlled to suit the particular experiment. Emission efficiencies can be high, even approaching 100% for positronium emission from some heated surfaces (Ref. [41] and references therein), since the positron implantation depth can be much less than its diffusion length.

In order to facilitate the production of antihydrogen by any of the schemes outlined in section 5, and its observation, it is preferable to have a pulsed positron or positronium source. This will involve the construction of a dedicated positron source and accumulator. A number of methods have been used to achieve this from radioactive source-based beams, as summarized in [41]. These include the electronic damping technique [42–44] and the buffer gas moderating scheme of Surko and co-workers [45, 46].

The latter method is by far the most efficient yet devised, and we plan to use a variant of this technique that incorporates accumulation under UHV conditions [47]. The trapping of the positrons is effected using an axial magnetic field for radial confinement and a system of appropriately biased electrodes which form a potential well for axial confinement. The source of slow positrons is a ^{22}Na radioactive source and a solid neon moderator [48] optimized for the positron accumulator. The neon moderator, which is grown at 8 K under computer control, is capable of providing a slow positron beam flux of 2×10^7 e^+/s from a 150 mCi (5.6 GBq) source [49]

Positrons from the beam are injected into the trap over a potential hill where they interact with the N_2 buffer gas. Around 30% of the positrons

lose sufficient kinetic energy to become trapped. After the initial trapping the buffer gas pressure is reduced to 5×10^{-10} Torr in less than 60 seconds, allowing storage times for the positrons in excess of 30 minutes. Using the solid neon moderated primary beam, a capture rate of 55,000 e^+/s per mCi of radioactive source has been achieved [49], as compared with only a few positrons per mCi for the electronic damping method [43,44].

The buffer gas trapping technique has achieved in excess of 10^8 positrons trapped in a vacuum of 5×10^{-10} Torr in a three minute cycle. With modest changes the buffer gas method can be further improved to allow accumulation of 10^{10} positrons per hour [47].

A schematic illustration of the set-up is shown in Fig. 1. The positron trapping sequence for the antihydrogen experiment has been described elsewhere [47]. It involves loading the trapping stage until equilibrium between the loading and annihilation rates is achieved, pumping out this stage to 5×10^{-10} Torr within one minute, and then opening valve A in Fig. 1 for a short period to allow the positrons to be transferred to the UHV storage stage. Once per hour, the accumulations of 10^{10} positrons can be shuttled to the cryogenic positron trap through the pulsed valve (B). An additional ultra-thin foil can be located at the entrance to the cryogenic section of the storage trap to avoid gas loading of the extreme high vacuum. Such foils typically have transmission efficiencies of $\sim 30\%$. Both the rapid pump down of the system (7 seconds per decade of pressure) and the transfer of positrons between various stages of the present accumulator have already been demonstrated experimentally [47].

5. Antihydrogen formation

5.1. Introduction

The initial focus of the ATHENA experiment is on the production and storage of antihydrogen atoms at very low energies. The recombination technique used in the ATHENA experiment should

- provide sufficient numbers of antihydrogen atoms for spectroscopy,
- produce the atoms at very low temperatures ($T \leq 1$ K) to allow trapping within achievable magnetic well depths,
- form antihydrogen atoms in the ground state or in low lying excited states, and
- achieve above with a reasonably fast reaction time.

Although a technique combining all these features has not yet been demonstrated, recent experimental results have been encouraging. In addition, measurements of recombination rates of protons and electrons in storage rings and experiments with crossed beams of protons and positronium give an experimental input to check the theoretical understanding of the recombination processes.

To form a bound state of antiproton and positron starting from free particles, excess energy and momentum has to be carried away by a third particle. Various schemes for producing antihydrogen have been proposed and discussed in some detail [28,51–56], with the first mentioning of the possible production of antihydrogen in traps by Dehmelt and co-workers [57].

The simplest process is spontaneous radiative recombination:

$$e^+ + \bar{p} \Rightarrow \overline{H} + h\nu \qquad (1)$$

(see references [58,59]). The rate for this process can be increased by laser stimulation [51]:

$$e^+ + \bar{p} + nh\nu \Rightarrow \overline{H} + (n-1)h\nu \; . \qquad (2)$$

A different approach is based on three-body collisions [28]:

$$e^+ + e^+ + \bar{p} \Rightarrow \overline{H} + e^+ \; . \qquad (3)$$

The above reactions require that two plasmas of opposite charge (antiprotons and positrons) are trapped and brought into contact. Alternatively, recombination by crossing a beam of positronium (either in the ground state or in low-lying excited states) with antiprotons has been proposed:

$$Ps + \bar{p} \Rightarrow \overline{H} + e^- \; , \qquad (4)$$

(see references [52,53]), and

$$Ps^* + \bar{p} \Rightarrow \overline{H^*} + e^- \ , \qquad (5)$$

(see references [54,55]).

In the following we discuss the basic principles of radiative and three-body recombination. Afterwards, the advantages and disadvantages of the proposed reactions are compared. In the absence of a proven scheme, we intend to pursue more than one route to trapped antihydrogen, with particular emphasis on the laser-stimulated recombination in nested traps and on the positronium-collision method.

5.2. Radiative recombination of positrons and antiprotons

Recombination between ions and electrons is an important issue in storage rings with electron cooling, since it causes significant beam losses. The measured rates of recombination, depending on the relative longitudinal and transverse velocity distributions of the two plasmas, can be used to estimate the corresponding rates in traps by considering the co-moving center-of-mass system of the ion (proton) beam.

The critical issues are the recombination rate and the initial state of the formed antihydrogen atom. Two processes are typically considered, spontaneous radiative recombination (SRR), and three-body recombination (TBR).

5.2.1. Spontaneous radiative recombination

The cross-section for spontaneous radiative recombination (SRR) [60] is related by time-reversal invariance to photo-ionization, and depends only on the kinetic energy E of the electron in the center-of-mass (c.m.) system of the proton, and the capture level n. The partial cross-section decreases with high n, and the total cross-section is obtained by summing over all n up to a "cut-off" level which is reached when antihydrogen atoms are ionized in collisions with neighboring atoms ($E \sim kT$) or by external electric fields. For example, an antihydrogen atom in an $n = 200$ state is ionized by electric fields of about 1 V/cm or by collisions with 0.34 meV kinetic energy. Typical cross-sections range from $5 \cdot 10^{-21}$ to $1.5 \cdot 10^{-16}$ cm^2 for relative kinetic energies of $E_{c.m.} \sim 1$ eV - 0.1 meV.

From these cross sections we can deduce the recombination coefficient α by integrating the product of cross section and velocity distribution over the spatial overlap of the two clouds. To get an order of magnitude for $\alpha(v_r)$, we consider the simple case where all velocities are equal:

$$\alpha(v_r) = \langle \sigma(v) v \rangle = \qquad (6)$$

$$\begin{cases} 3.2 \cdot 10^{-13} \ \ cm^3 s^{-1} \ \ (1eV) \\ 7.1 \cdot 10^{-12} \ \ (10meV) \\ 0.9 \cdot 10^{-10} \ \ (0.1meV) \end{cases} \qquad (7)$$

These values agree within a factor 2 or better with more elaborate calculations [61] as well as with experiments at the Test Storage Ring (TSR) in Heidelberg [62].

To find the rates for spontaneous recombination in a nested Penning trap, we have to make some assumptions about the relative velocity distributions of the electron and the proton cloud and the spatial overlap of their distribution functions. An upper limit for recombination rates can be obtained by assuming a complete overlap of proton and electron clouds, characterized by an average relative velocity v_r.

With $N_e = 10^8$, $N_p = 10^7$, and using the approximate value of $\alpha(v)$ in (7), the upper limits for the spontaneous recombination rates at different electron energies are: $R = 300$ s^{-1} (1 eV), 7000 s^{-1} (10 meV), and 90.000 s^{-1} (0.1 meV). respectively.

5.2.2. Laser-induced radiative recombination

The rate for spontaneous radiative recombination is small since the emission of a photon, necessary to conserve energy and momentum, is a slow process on the time scale of a collision. Therefore laser-induced recombination (see reaction (2) and reference [51]) was proposed, in which the capture rate in particular $n-$states would be increased by illuminating the reaction region with photons of appropriate energy $h\nu$ corresponding to the particular continuum to bound-state transition. Laser-stimulated recombination of protons

with electrons in continuum states has been studied extensively at storage rings, and has been discussed in several papers [63]. A measure for the efficiency of laser-stimulated recombination is the ratio of the induced recombination rate to the total spontaneous recombination rate, the enhancement factor G.

For a maximum enhancement factor, a low energy spread in the electron (positron) energy distribution and a high laser power density are most important. The limiting effect is photo-ionization of the produced (anti)hydrogen atoms, leading to saturation of the enhancement factor when the laser intensity is increased. At the TSR in Heidelberg, proton-electron recombination into n=2 has been studied at laser pulse intensities close to 20 MW/cm^2, leading to an enhancement factor G = 70 ±2, not far from the expected enhancement factor of 85 [64].

5.2.3. Three-body recombination in dense positron plasmas

This mechanism, where three particles (two positrons and an antiproton) collide simultaneously, only plays a role at high positron densities and low temperatures. The rate for three-body recombination $\alpha_{TBR}(n)$ as a function of the capture level n has been calculated [65] by considering the time-reversed process, i.e. electron-impact ionization of hydrogen, which is well known:

$$\alpha_{TBR}(n) = \frac{1.96 \cdot 10^{-29} cm^6 s^{-1} n_e}{(kT/eV)} \, n^6 \qquad (8)$$

The steep dependence on the principal quantum number n indicates that mostly very high Rydberg states close to the "cut-off" level $n^* \sim \sqrt{R/2kT}$ ($R = 13.6$ eV) are populated. Summing up all contributions from n=1 to n^*, the total three-body recombination rate for a Maxwellian positron velocity distribution of temperature T becomes:

$$\alpha_{TBR}(n^*) = \frac{2.7 \cdot 10^{-27} cm^6 s^{-1}}{(kT/eV)^{4.5}} \, n_e \qquad (9)$$

This formula is in excellent agreement with previously quoted results [66]. A comparison with the recombination coefficient for radiative recombination shows that for positron densities $n_e = 10^6$ cm^{-3} three-body recombination becomes comparable at $kT \sim 10$ meV, and then increases by 4.5 orders of magnitude per factor 10 of decreasing temperature. Consequently, at very low temperatures this process is expected to dominate completely and a dynamic equilibrium will be reached, with as many antihydrogen atoms forming in high-n as are destroyed by collisions or field ionization. Only if an effective deexcitation mechanism is used to induce transitions to lower lying states, which then decay rapidly to the ground state, will this process be useful for the purpose of antihydrogen formation for precision spectroscopy. The positrons captured in high-lying bound levels can be stabilized by stimulating a transition to lower levels, i.e. the 11.1 μm light of a $^{13}CO_2$ laser could be used to drive a transition to n = 11.

5.3. Positronium-antiproton collisions

Collisions between antiprotons and positronium atoms (reactions 4 and 5) have also been proposed as a possible recombination scheme [30, 53].The relevant cross-section can be derived from the related process of positronium formation in positron-atomic hydrogen collisions. A summary of calculations and data has been given by Ermolaev [67]. He stresses that recent calculations [68] have found cross-sections for antihydrogen formation of 10^{-15} cm^2 for positronium impact energies of a few electron-volts. These calculations also show that antihydrogen is produced mostly in the ground or first excited state, given that the positronium is in its ground state.

It was pointed out some time ago [54] that the use of excited state positronium atoms for antihydrogen production (reaction 5) had some advantages over the use of the ground state. Notably, the cross-section was argued to follow a classical area scaling law (proportional to the fourth power of the positronium principal quantum number) and is therefore expected be much enhanced. (This has been supported by quantum mechanical calculations [68].) Again the antihydrogen is formed into relatively low-lying states such that, as argued by Deutch *et al.* [55], the

recoil energy of the excited antihydrogen can be low.

6. Magnetic traps for antihydrogen

Having discussed the generation, trapping of all necessary components, and possible recombination schemes whereby antihydrogen can be formed, the next task is to combine all this into an environment suitable for trapping and studying the neutral antihydrogen atoms.

To confine neutral atoms the force exerted by the magnetic gradient onto the magnetic moment of the neutral atoms may be used. This separates the (anti-)hydrogen into low-field seeking and high-field seeking atoms. The trap configuration used to radially confine the low-field seeking atoms normally consists of an arrangement of coils known as Ioffe-Pritchard trap [32] , designed to produce a magnetic minimum at the center of the trap without having a zero field location, which would introduce spin-depolarizing Majorana transitions. Axial confinement is typically achieved through coaxial solenoids at either end of the trapping volume, which provide a barrier against axial leakage and also the non-zero field value in the center. Ioffe-Pritchard magnetic traps have been successfully used by the groups at MIT [33] and in Amsterdam [69]. Typically trap depths of 1K were achieved .

The proposed static magnetic trap for the ATHENA apparatus is a modified version of the Ioffe-Pritchard configuration designed with the goal of achieving the highest possible trap depth while allowing room for the particle detection system and the antiproton trap. In our apparatus the trap consists of four superconducting race-track "quadrupole" coils and one solenoid (compensation solenoid) running oppositely to the main solenoid to generate a field minimum in the axial direction.

When working with hydrogen, magnetic traps are filled by allowing the hydrogen "gas" to fall into the potential well by inelastic collisions with residual gas atoms and the walls, a method unacceptable for antihydrogen. Therefore we propose to superimpose the magnetic trap onto the Penning and/or combined trap to be used for the recombination process in such a way that the antihydrogen formation takes place in the minimum of the magnetic well. Antihydrogen produced in the high-field seeking states will quickly leave the trap volume, while the low-field seeking states would be repelled by the magnetic barrier and, if the well depth is higher than the kinetic energy of the formed atoms, will be trapped.

7. Physics with antihydrogen

7.1. High resolution spectroscopy

A central goal of the ATHENA collaboration is to compare the level structure of antihydrogen with that of hydrogen with the highest possible precision. The most interesting spectroscopy is the two-photon 1S-2S transition at the excitation wavelength of 243 nm, half the Lyman-α frequency, with a natural linewidth of 1.3 Hz. This linewidth represents an accuracy of 5 parts in 10^{16}, which, with a sufficiently high signal-to-noise ratio, could be enhanced to 1 part in 10^{18} by determining the line center to high accuracy.

The group of T. W. Hänsch in Munich [70] has been performing high precision spectroscopy on hydrogen for the last twenty years, using a cold atomic beam traveling collinear to a standing wave light field. This method is intrinsically free of the first order Doppler effect, and the accuracy was limited by the second-order Doppler effect due to the thermal velocity spread of the atoms. By actively selecting the low velocity component of the beam, the narrowest line achieved with this method so far has been about 3 kHz wide, representing a relative accuracy of 2.8×10^{-12} [71]. At MIT, a record relative resolution of 2 parts in 10^{12} with a high signal-to-noise ratio in this transition has recently been achieved [72] by using cold, trapped hydrogen atoms. The limitations of this experiment were the laser frequency instabilities and the lack of a good reference standard to which the laser frequency can be locked.

Laser spectroscopy of antihydrogen will require in many respects a rather different technology from what has been used so far with hydrogen. Experiments will have to be carried out in the comparatively harsh environment of an accelerator. The first improvement would be the replace-

ment of the sensitive dye laser system by a frequency doubled Ti:Sapphire laser, operating at 972 nm. In the future it may become possible to start with a high power diode laser at 972 nm, eliminating the need for large Ar^+ or Kr^+ ion pump lasers. A similar development will be necessary in terms of providing a smaller and more robust hydrogen frequency standard.

An additional complication in performing spectroscopic experiments on trapped antihydrogen is the relatively small number of atoms available. Unlike in beam experiments, where a continuous stream of hydrogen atoms can be used, or in the trapped hydrogen experiments at MIT in dense samples, most efficient use of the antihydrogen atoms is required. The excitation of atoms to the 2S level is typically detected through field-induced Lyman-α fluorescence. Both the quenching field and the spontaneous L_α emission will cause spin flips and cause the atoms to leave the trap. This can be avoided by using a microwave transition to cycle the atom through the $2P_{3/2}, F = 2, m = 2$ state, ensuring that the atom always decays back into the low-field seeking ground state.

Additionally, the power in the VUV light necessary to excite the 1S-2S transition may cause photo-ionization of the n=2 level, representing another loss mechanism. Zimmermann [73] estimates the number of atoms needed for high-resolution spectroscopy. By balancing the need for minimizing the photo-ionization losses by a fast quenching rate against the unavoidable line broadening introduced by quenching, he estimates that with 1000 atoms at 0.2 K a fractional accuracy in determining the center of the line would be better than 1 part in 10^{12}, if the Zeeman-broadening and the quench-broadening are both kept at about 20 kHz.

Such an accuracy exceeds the currently available CPT tests of the electromagnetic interaction by 2 orders of magnitude. Further improvements, eventually up to a fractional accuracy of 1 part in 10^{18}, appear feasible, in principle, but will require many further technical developments, including efficient cooling of antihydrogen atoms in the trap.

7.2. Gravity studies on antimatter

If spectroscopic comparisons of antihydrogen to hydrogen would yield a difference, this would not necessarily constitute a violation of CPT, but could also be interpreted as an anomalous redshift of the antiatom. Hughes [74] has studied the consequence of an anomalous gravitational coupling to antimatter, with a range larger than the distance of the Earth to the Sun, but smaller than our galaxy. Assuming exact CPT symmetry and a tensor force gravitational interaction with infinite range, he showed that a comparative measurement of the 1S-2S transition frequency in hydrogen and antihydrogen at a level of 1 part in 10^{15} would test the weak equivalence principle for positrons at a level of 1 part in 10^{11}. Such tests are not model-independent and would require a variety of further experiments to distinguish between possible violations of CPT or the weak equivalence principle. Therefore, direct measurements would be preferable and would yield valuable complementary information, albeit with lower precision. Such experiments could comprise free-fall experiments [75], measurements of the gravitational sag of a stored antihydrogen cloud [76], or interferometric methods [77,78].

8. Summary

We have described the necessary steps to obtain the ingredients and the possible scenarios to form antihydrogen atoms at rest for precision spectroscopy. While it may take many years of intense work to reach the ultimate accuracy of 1 part in 10^{18}, current technology will allow the comparison of hydrogen and antihydrogen atoms at a level of 1 part in 10^{12}. Such a measurement would represent an improvement of known tests of CPT for baryons. With recent advances in the theoretical understanding of possible mechanisms and implications of CPT violations such tests are of critical importance to the further development of physics and well justify the construction of a dedicated antiproton source.

REFERENCES

1. G. Lüders; Kong. Danske Vidensk. Selsk.

Mat.-Fys. Medd. 28 No. 5 (1954) 1; Ann. Phys. 2 (1957) 1.
2. W. Pauli; in: *Niels Bohr and the Development of Physics*, ed. by W. Pauli (Pergamon, New York, 1955), p. 30.
3. J. S. Bell; Proc. Roy. Soc. A 231 (1955) 479.
4. R. Jost; Helv. Phys. Acta 30 (1957) 409; *The General Theory of Quantized Fields* (American Mathematical Society, Providence, Rhode Island, 1965).
5. J. J. Sakurai; *Invariance Principles and Elementary Particles* (Princeton University Press, Princeton, 1964); R. F. Streater and A. S. Wightman, *PCT, Spin & Statistics, and All That* (Benjamin, New York, 1964).
6. Particle Data Group; Phys. Lett. B204 (1988) 46
7. R. S. Van Dyck, P. B. Schwinberg, and H. G. Dehmelt; Phys. Rev. Lett. 59 (1987) 26.
8. G. Gabrielse, D. Phillips, W. Quint, H. Kalinowsky, and G. Rouleau; Phys. Rev. Lett. 74 (1995) 3544.
9. V. A. Kostelecky and R. Potting; Nucl. Phys. B359 (1991) 545;
10. P. Huet and M. Peskin; Nucl. Phys. B434 (1995) 3
11. A. Kostelecky and R. Potting; Phys. Rev. D51 (1995) 3923
12. D. Colladay and A. Kostelecky; Phys. Lett. B344 (1995) 259;
13. J. Ellis, J. Lopez, N. Mavromatos and D. Nanopoulos; CERN-TH/95-99;
14. D. Colladay and A. Kostelecky; Phys. Rev. D 52 (1995) 6224
15. R. Adler *et al.* (CPLEAR) and J. Ellis, J. Lopez, N. Mavromatos and D. Nanopoulos; CERN-PPE/95-149
16. T. Prokopec, R. Brandenberger, A. Davis and M. Trodden; CLNS 95/1368, hep-ph/9511349;
17. J. Ellis, N. Mavromatos and D. Nanopoulos; CERN-TH/96-189
18. P. Huet; UW/PT 96-11, hep-ph/9607435;
19. A. Kostelecky and R. van Kooten; accepted for publication in Phys. Rev. D;
20. A. Kostelecky; Talk at PANIC '96, May 1996, hep-ph/9607482;
21. D. H. MacIntyre and T. W. Hänsch; Metrologia 25 (1988) 61.
22. M. Charlton, J. Eades, D. Horvath, R. J. Hughes, and C. Zimmermann; Phys. Rep. 241 (1994) 65.
23. R. J. Hughes, M. H. Holzscheiter; Journal of Modern Optics 39 (1992) 263.
24. M. M. Nieto and T. Goldman; Phys. Rep. 205 (1991) 221-281; and Phys. Rep. 216 (1992) 343
25. M. H. Holzscheiter; Physica Scripta T59 (1995) 326
26. S. Maury, *et al.*; CERN/PS 96-43 (AR)
27. Guo-Zhong Li, R. Poggiani, G. Testera, G. Torelli, and G. Werth; Hyperfine Int. 76 (1993) 343
28. G. Gabrielse, S. L. Rolston, L. Haarsma, and W. Kells; Phys. Lett. A129 (1988) 38
29. J. Walz, S. B. Ross, C. Zimmermann, L. Ricci, M. Prevedelli, and T. W. Hänsch; Phys. Rev. Lett. 75 (1995) 18
30. J. W. Humbertson, M. Charlton, F. M. Jacobsen, B. I. Deutch; J. Phys. At. Mol. Phys. B20 (1987) L25
31. Y. V. Gott, M. S. Ioffe, V. G. Tel'kovskii; Nucl. Fusion, 1962 suppl., Pt. 3 (1962) 1045
32. D. E. Pritchard; Phys. Rev. Lett. 51, 1336 (1983).
33. C. L. Cesar, D. Fried, T. Killian, A. Polcyn, J. Sandberg, I. A. Yu, T. J. Greytak, D. Kleppner, and J. M. Doyle; Phys. Rev. Lett. 77 (1996) 255
34. F. Schmidt-Kaler, D. Leibfried, M. Weitz, T. W. Hänsch; Phys. Rev. Lett. 70 (1993) 2261
35. G. Gabrielse, X. Fei, L. A. Orozco, R. L. Tjoelker, J. Haas, H. Kalinowsky, T. A. Trainor, W. Kells; Phys. Rev. Lett 63 (1989) 1360
36. M. H. Holzscheiter, X. Feng, T. Goldman, N. S. P. King, R. A. Lewis, M. M. Nieto, G. A. Smith; Phys. Lett. A 214 (1996) 279
37. G. Gabrielse, L. Haarsma, and S. L. Rolston; Int. J. Mass Spec. and Ion Processes 88 (1989) 319
38. G. Gabrielse, X. Fei, L. A. Orozco, R. L. Tjoelker, J. Haas, H. Kalinowsky, T. A. Trainor, and W. Kells; Phys. Rev. Lett 65 (1990) 1317
39. W. Thompson and S. Hanrahan; Jour. Vac.

Sci. Tech. 14 (1977) 643
40. P. J. Schultz and K. G. Lynn; Rev. Mod Phys.. 60 (1988) 701
41. M. Charlton and G. Laricchia; Hyperfine Int. 76 (1993) 97
42. P. B. Schwinberg, R. S. VanDyck and H. Dehmelt; Phys. Lett. A81 (1981) 119
43. L. Haarsma, K. Abdullah and G. Gabrielse; Phys Rev Lett 75 (1995) 806
44. D. S. Hall, G. Gabrielse; Phys. Rev. Lett. 77 (1996) 1962
45. T. J. Murphy, C. M. Surko; Phys. Rev. A46 (1992) 5696
46. R. G. Greaves, M. D. Tinkle, C. M. Surko; Phys. Plasmas 1 (1994) 1439
47. C.M. Surko, R.G. Greaves and M. Charlton; to be published in Hyperfine Int.
48. A. P. Mills, Jr., and E. M. Gullikson; Appl. Phys. Lett. 49 (1996)
49. R. G. Greaves and C. M. Surko; Can. J. Phy. 74 (1996) 445
50. R. Neumann, H. Poth, A. Wolf, and A. Winnacker; Z. Phys. A313, 253 (1984)
51. B. I. Deutch, F. M. Jacobsen, L. H. Andersen, P. Hvelplund, H. Knudsen, M. H. Holzscheiter, M. Charlton, G. Laricchia; Phys. Scrip. T22, 288 (1988)
52. B. I. Deutch, L. H. Andersen, P. Hvelplund, F. M. Jacobsen, H. Knudsen, M. H. Holzscheiter, M. Charlton, and G. Laricchia; Hyperfine Int. 44, 271 (1988)
53. M. Charlton; Phys. Lett. A143, 143 (1990)
54. B. I. Deutch, M. Charlton, M. H. Holzscheiter, P. Hvelplund, L. V. Jørgensen, H. Knudsen, G. Laricchia, J. P. Merrison, and M. R. Poulsen; Hyperfine Int. 76 (1993) 153
55. C. T. Munger, M. Mandelkern, J. Schultz, G. Zioulas, T. A. Armstrong, M. A. Hasan, R. A. Lewis, and G. A. Smith; Proposal to Fermilab (1992)
56. H. Dehmelt, R. Van Dyck, P. Schwinberg, and G. Gabrielse; Bull. Am. Phys. Soc. 24, 757 (1979)
57. G. Budker and A. Skrinsky; Sov. Phys.-Usp. 21, 277 (1978)
58. H. Herr, D. Möhl, and A. Winnacker; in *Proc. 2nd Workshop on Physics with Cooled Low Energy Antiprotons at LEAR*, Erice, May 9-16. 1982. (eds. U. Gastaldi and R. Klapisch) p. 659. Plenum, New York 1984
59. H. A. Bethe and E. E. Salpeter; *Quantum Mechanics of One- and Two- Electron Atoms*, Springer Verlag, Berlin (1957)
60. M. Bell. J. S. Bell; Part. Acc. 12 (1982) 49
61. A. Wolf *et al.*; Z. Phys. D21 (1991) 69
62. A. Wolf; Hyperfine Int. 76 (1993) 189, and ref. therein
63. U. Schramm, J. Berger, M. Grieser, D. Habs, E. Jaeschke, G. Kilgus, D. Schwalm, A. Wolf, R. Neumann, R. Schuch; Phys. Rev. Lett. 67 (1991) 22
64. M. Pajek, R. Schuch; to be published; Poster at the 2nd Euroconference on Atomic Physics with Highly Charged Ions, Stockholm, June 1996
65. P. Mansbach, B. Keck; Phys. Rev. 181 (1969) 275
66. A. M. Ermolaev; Hyperfine Int. 100 (1996) 41
67. J. Mitroy and A. T. Stelbovics; J. Phys. B27 (1994) L79, and priv. comm.
68. I.Setija, H.Werij, O.Luiten, M.Reynolds, T.Hijmans, J.Walraven; Phys. Rev. Lett. 70 , 2257 (1993)
69. M. Weitz, A. Huber, F. Schmidt-Kaler, D. Leibfried, and T. W. Hänsch; Phys. Rev. Lett. 72 (1994) 328
70. D. Leibfried; PhD Thesis, MPI Munich, August 1995
71. C. Cesar *et al.*; in *Proceedings of the Fifth Symposium on Frequency Standards and Metrology* ed. J. Bergquist, Cape Cod (1995) World Scientific
72. T. W. Hänsch, C. Zimmermann; Hyperfine Int. 76 (1993) 47
73. R. J. Hughes, M. H. Holzscheiter; J. Mod. Optics 39 (1992) 263
74. N. Beverini, V. Lagomarsino, G. Manuzio, F. Scuri, and G. Torelli; Hyperfine Int. 44 (1988) 349
75. R. Poggiani; Hyperfine Int. 76 (1993) 371
76. T. J. Phillips; in *Low Energy Antiproton Physics, LEAP '94*, eds. G. Kernel *et al.*; World Scientific (1995) 589
77. M. Kasevich and S. Chu; Appl. Phys. B 54 (1992) 321